

Visualization of *NRAS* RNA G-Quadruplex Structures in Cells with an Engineered Fluorogenic Hybridization Probe

Shuo-Bin Chen,[†] Ming-Hao Hu,[†] Guo-Cai Liu,[†] Jin Wang,[‡] Tian-Miao Ou,[†] Lian-Quan Gu,[†] Zhi-Shu Huang,^{*,†} and Jia-Heng Tan^{*,†}

[†]School of Pharmaceutical Sciences, Sun Yat-sen University, Guangzhou 510006, China

[‡]Guangzhou Institute of Geochemistry, Chinese Academy of Sciences, Guangzhou 510640, China

Supporting Information

ABSTRACT: The RNA G-quadruplex is an important secondary structure formed by guanine-rich RNA sequences. However, its folding studies have mainly been studied *in vitro*. Accurate identification of RNA G-quadruplex formation within a sequence of interest remains difficult in cells. Herein, and based on the guanine-rich sequence in the 5'-UTR of *NRAS* mRNA, we designed and synthesized the first G-quadruplex-triggered fluorogenic hybridization (GTFH) probe, ISCH-*nras1*, for the unique visualization of the G-quadruplexes that form in this region. ISCH-*nras1* is made up of two parts: The first is a fluorescent light-up moiety specific to G-quadruplex structures, and the second is a DNA molecule that can hybridize with a sequence that is adjacent to the guanine-rich sequence in the *NRAS* mRNA 5'-UTR. Further evaluation studies indicated that ISCH-*nras1* could directly and precisely detect the targeted *NRAS* RNA G-quadruplex structures, both *in vitro* and in cells. Thus, this GTFH probe was a useful tool for directly investigating the folding of G-quadruplex structures within an RNA of interest and represents a new direction for the design of smart RNA G-quadruplex probes.

Since RNA can fold onto itself and form fully paired regions or noncanonically paired regions,¹ such RNA secondary structures are crucial for gene regulation and function.² In the past years, RNA folding processes have been investigated in detail.³ However, most experiments were performed *in vitro*. Only a few methods can be directly applied to investigate RNA structures in the cell, and even fewer for noncanonical RNA structures.⁴

RNA G-quadruplexes (G4s) are noncanonical secondary structures that are formed by guanine-rich (G-rich) RNA sequences via stacking of hydrogen-bonded G-quartets.⁵ Computational searches for potential RNA G-quadruplexes have identified an overrepresentation of these structures in the untranslated regions (UTRs) of mRNAs and in long noncoding RNAs.⁶ Accumulating evidence suggests that RNA G-quadruplexes play important functional roles in the control of a variety of cellular processes.⁷ Thus, studying the structure–function relationships of RNA G-quadruplexes has attracted considerable attention.

Similar to the problems encountered while studying RNA secondary structures, approaches for identifying RNA G-

quadruplexes have been largely limited to some *in vitro* biophysical techniques and computational prediction methods.⁸ The current *in vitro* studies are not sufficient to understand how these RNAs fold and function in their native environment in the cell, which is densely crowded.⁹ Notably, several fluorescent probes and antibodies have been developed to investigate RNA G-quadruplexes.¹⁰ However, these molecules are not able to distinguish between different RNA G-quadruplexes, as they label all of the potential RNA G-quadruplexes in cells. Accordingly, there are no molecular probes that can selectively determine a particular G-quadruplex structure formed by specific G-rich RNAs of interest. Such technical difficulties greatly restrict specific investigations on the structure–function relationships of various RNA G-quadruplexes.

We recently developed an isaindigotone-based fluorescent light-up probe specific for G-quadruplex structures, but its selectivity for different G-quadruplexes was not satisfactory.¹¹ Therefore, we are interested in modifying this probe to develop a much smarter molecule that can individually visualize G-quadruplex structures formed by G-rich sequences of interest. Currently, one of the most common methods for detecting and localizing specific RNAs in cells is fluorescence *in situ* hybridization (FISH) techniques that use fluorescent probes that bind to parts of particular sequences with a high degree of sequence complementarity.¹² Enlightened by the idea of the FISH technique, we determined that attaching an oligonucleotide (anti-tail sequence) that could hybridize with a sequence that is adjacent (tail sequence) to the G-rich sequence of interest in ISCH-1 would be a designable approach to improve our probe's selectivity. As shown in Figure 1A, we expect that the oligonucleotide will force the fluorophore located beside the defined G-rich sequence to trigger its fluorescent signal upon binding to the G-quadruplex structure. Thus, we called this engineered molecule a G-quadruplex-triggered fluorogenic hybridization (GTFH) probe.

The GTFH probe was designed to contain the following two parts: (1) the fluorescent light-up moiety derived from ISCH-1 for identifying the G-quadruplex and (2) an oligonucleotide for directing hybridization. Accordingly, an alkyne side chain was first introduced onto ISCH-1 to create the new molecule ISCH-*oa1* (Figure 1B, Scheme S1 and Figures S1–S4). This modification enabled a convenient and accessible conjugation

Received: May 10, 2016

Published: August 10, 2016

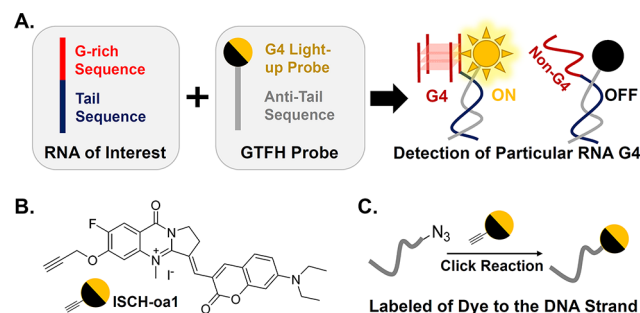


Figure 1. Illustration of GTFH probe. (A) GTFH probe design principle. (B) Chemical structure of ISCH-oo1. (C) GTFH probe preparation.

process with commercially purchased azido-modified oligonucleotides via a click reaction (Figure 1C).

To test the application of the GTFH probe, the most studied G-rich sequence, G4T2S, which is located in the 5'-UTR of the NRAS mRNA, was chosen as the target (Figure 2).¹³ The first

NRAS mRNA	GRS	TS	5' UTR	Encoding Sequence
RNAs	G-Rich Sequence (GRS)	Tail Sequence (TS)		
G4T2S	5'-UGUGGGAGGGCGGGUCUGGG	UGCGGCCUGCCGCAUGACUCGUGGU-3'		
G4T25-mg1	5'-UGUAAAGAGAGCGAGUCUGAG	UGCGGCCUGCCGCAUGACUCGUGGU-3'		
G4T25-mg2	5'-UGUAAAAAAGCGAGUCUGAG	UGCGGCCUGCCGCAUGACUCGUGGU-3'		
G4T25-mt1	5'-UGUGGGAGGGCGGGUCUGGG	UACAACCUACCAUAUCUCAUAU-3'		
G4d	5'-UGUGGGAGGGCGGGUCUGGG	-3'		
GT2S	5'-G	UGCGGCCUGCCGCAUGACUCGUGGU-3'		
Probes	Fluorescent Label for Detection	Anti-Tail Sequence (ATS)		
ISCH-nras1	G4 Light-Up	ISCH-oo1 3'-ACGCCGGACGGGTACTGAGCACCA-5'		
ISCH-r1	Fluorophore	ISCH-oo1 3'-ATCCACATCACTTCGCATCAGCTA-5'		
A647-nras1	Marker	Alexa Fluor 647-3'-ACGCCGGACGGGTACTGAGCACCA-5'		

Figure 2. Illustration of G-rich RNA sequences and the related GTFH probes used in this study.

GTFH probe, ISCH-nras1, which included an ISCH-oo1 labeled on the 3'-end of a 25-mer DNA sequence complementary to the nearby downstream tail sequence of the G-rich sequence on G4T2S, was then designed and synthesized through a click reaction. A negative reference called ISCH-r1, whose anti-tail sequence was mutated to prevent hybridization, was also prepared (Scheme S2, Table S1, and Figures S5–S6). In addition to G4T2S, RNAs with mutations (G4T25-mg1 and G4T25-mg2) and deletion (GT2S) of the G-rich sequence, as well as a mutation (G4T25-mt1) and deletion (G4d) of the tail sequence, were also used as controls. CD, TDS, and EMSA studies demonstrated that only G4T2S, G4T25-mt1, and G4d could form G-quadruplex structures, and the probe ISCH-nras1 could hybridize with G4T2S, G4T25-mg1, G4T25-mg2 as well as GT2S (Figures S7–10).

The fluorescence properties of ISCH-nras1 with different RNAs were initially investigated by fluorescence spectroscopy *in vitro* (Figure S11). As shown in Figure 3, ISCH-nras1 alone in buffer displayed weak emission. An emission peak at ~650 nm appeared and was significantly enhanced upon gradual addition of the RNA G-quadruplex formed by the G4T2S. Concentration-dependent experiments indicated that the detection limit of ISCH-nras1 for G4T2S in solution was 0.024 μ M (Figure S12). In contrast, we observed a much weaker fluorescent enhancement or even a decrease in signal when the G4T25-mg1, G4T25-mg2, GT2S, G4T25-mt1, G4d RNAs and other G-quadruplexes were used (Figure S13). Furthermore, in the control experiments, negligible fluorescent enhancement was observed upon addition of G4T2S into the negative reference ISCH-r1 (Figure S14A). In contrast, the

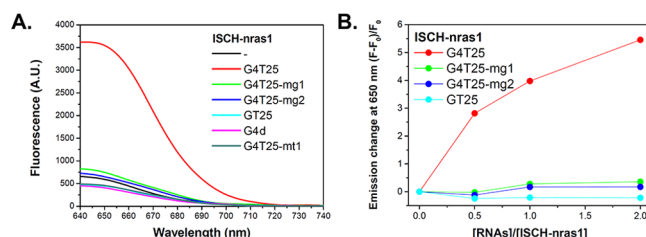


Figure 3. Fluorescence spectrum of ISCH-nras1 with RNAs. (A) Fluorescence spectrum of 1 μ M ISCH-nras1 with or without 2 μ M RNAs. (B) Fluorescence emission change of 1 μ M ISCH-nras1 at 650 nm against the ratio of [RNAs]/[ISCH-nras1] at λ_{ex} = 630 nm.

fluorescence of the precursor fluorophore ISCH-oo1 was greatly enhanced by the G4T2S, G4T25-mt1 RNAs and other G-quadruplex structures (Figures S15–S16). Accordingly, these results confirmed that attaching an oligonucleotide to the G-quadruplex probe that could hybridize with a sequence adjacent to the G-rich sequence of interest would improve its selectivity. To further confirm that the ISCH-nras1 emission originated from the G-quadruplex structure, we incubated ISCH-nras1 with G4T2S in several G-quadruplex unfolding conditions.¹⁴ The ISCH-nras1 emissions in these conditions were obviously weak (Figures S14B, S17–S18). Taken together, the results show that the ISCH-nras1 probe has promise for the selective detection of NRAS RNA G-quadruplex.

Encouraged by the *in vitro* results, we prepared to transfect the ISCH-nras1 into cells. In view of the extremely low concentration of a particular RNA in a single cell, targeted RNA secondary structure detection in cells can be achieved by either amplifying the fluorescent signal or transfecting the RNA of interest into cells.^{12a,15} At this stage, we chose to transfect the RNAs that we used in the *in vitro* experiments into cells to further validate the performance of ISCH-nras1 (Figure 4A). The conventional FISH probe A647-nras1 (Figure 2) was used as a marker to study the transfection efficiency and hybridization activity in cells.

As shown in Figure 4B, upon transfection of the RNAs containing the native tail sequence, the cell samples stained by A647-nras1 exhibited strong fluorescent spots in the cytoplasm. The approximate number of spots for A647-nras1

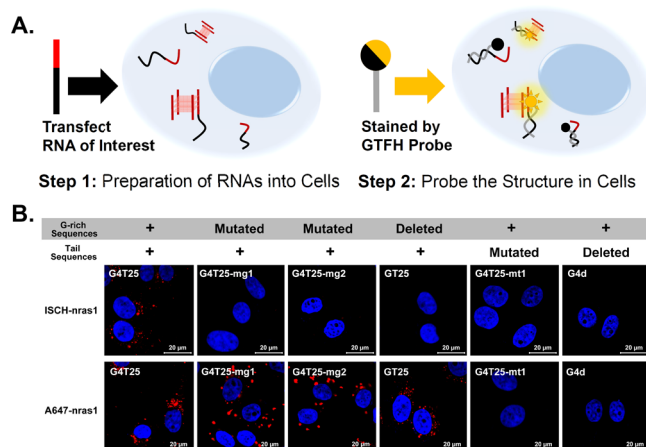


Figure 4. Detection of the targeted RNA G-quadruplexes inside cells. (A) Illustration of the transfection and tracking of the RNAs inside cells. (B) Confocal imaging of RNA-transfected cells stained with ISCH-nras1 and A647-nras1.

among the different cell samples revealed similar and stable transfection efficiency under our experimental conditions (Figure S19). Then, the cell samples were stained with ISCH-nras1. Remarkably, fluorescent spots were observed only in the cell samples containing G4T25, and not in the cells containing G4T25-mg1, G4T25-mg2, or GT25. This result was consistent with the *in vitro* fluorescence studies, showing that ISCH-nras1 exhibits considerable selectivity for the G-quadruplex formed by G4T25. Notably, no fluorescent signal was observed in the cells transfected with G4T25-mt1 or G4d and stained with A647-nras1 and ISCH-nras1, suggesting the complementary sequence is crucial for recognition. To better understand their hybridization in cells, RNase A and H digest experiments were conducted in the cells transfected with G4T25 (Figure S20).¹⁶ The original enhanced fluorescence signals due to A647-nras1 and ISCH-nras1 in the cytoplasm clearly disappeared after RNase A and H treatment. The addition of the complementary strand P25c to the tail sequence of G4T25 in the staining processes also resulted in the disappearance of the fluorescent signals (Figure S21). The ISCH-r1 and ISCH-oa1 probes that could not hybridize with the tail sequence of G4T25 also showed negligible fluorescence in the experiments (Figure S22). Taken together, these results confirmed that hybridization occurred between ISCH-nras1 and G4T25 inside cells and that ISCH-nras1 can be used to visualize the specific G-quadruplex structures formed by this G-rich sequence.

To further ascertain the ISCH-nras1 emission originated from its fluorescent light-up moiety binding to G-quadruplex structure in cells (Figure S23A), the complementary strand G4c to the G-rich sequence and the ligand IZCM-7, which binds to the NRAS G-quadruplex (Figure S24), were used to unfold the G-quadruplex and displace the ISCH-nras1 light-up moiety from the targeted G-quadruplex structure, respectively.¹⁷ The original enhanced fluorescence due to ISCH-nras1 in the cytoplasm gradually decreased after G4c or IZCM-7 treatment (Figure S23B). Accordingly, these results confirmed the function of the G-quadruplex light-up moiety in the GTFH probe.

Aside from its sensing mechanism, the selectivity of ISCH-nras1 was also confirmed by a competition assay, in which we tested the ability of ISCH-nras1 to retain enhanced fluorescence emission by cotransfecting cells with G4T25 and the abundant G-rich competitors (Figures S25–S26).¹⁸ In the assay, G4T25 was labeled with FAM for tracking in cells. In the presence of various amounts of competitor, the enhanced fluorescence of ISCH-nras1 with the G-quadruplex formed by G4T25 was only slightly affected. Overlap with the FAM-labeled G4T25 was evident. These results demonstrate the promising potential of ISCH-nras1 to serve as a highly selective probe for the specific G-quadruplex structure formed by the G4T25, even in harsh competitive environments.

The full-length NRAS 5'-UTR RNA contains 254 nucleotides, which is much longer than the G4T25 sequence. We are curious to know whether ISCH-nras1 could be applied to detect the G-quadruplex structure within the full-length RNA because previous nucleic acid probes labeled with FRET fluorophores or pyrene excimers could not achieve this goal.¹⁹ To this end, full-length NRAS 5'-UTR RNAs (UTR-full) were prepared as validation models and transfected into cells. Aside from UTR-full, long RNAs with a mutation (UTR-mutG) or deletion (UTR-delG) of the G-rich sequence, as well as a mutation (UTR-mT25) of the tail sequence, were also used as

controls. As shown in Figure 5, only cells transfected with UTR-full could be stained by ISCH-nras1. Mutation or

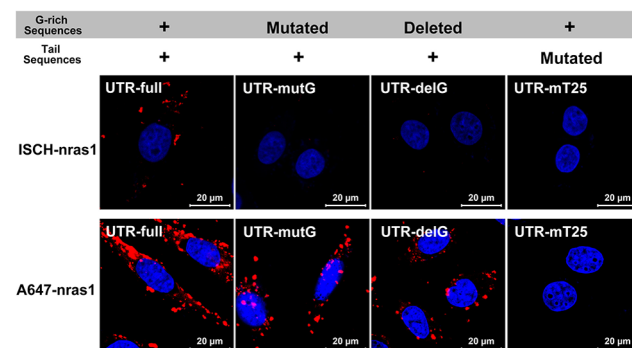


Figure 5. Confocal imaging of cells transfected with long RNAs and stained with ISCH-nras1 and A647-nras1.

deletion of the G-rich sequence in full-length RNA inhibited the fluorescence signal. By contrast, the cell samples stained with A647-nras1 exhibited strong fluorescence spots in the cytoplasm. Additionally, no fluorescent signal was observed when the cells containing UTR-mT25 were treated with ISCH-nras1 and A647-nras1. These findings are consistent with the results observed from the above staining assays, showing that ISCH-nras1 displays practical and promising application prospects for the selective detection of the specific G-quadruplex formed by the G-rich sequence within the short and long forms of the NRAS mRNA 5'-UTR.

In summary, we have successfully developed the first GTFH probe, ISCH-nras1, for the unique visualization of the G-quadruplex structure formed by the G-rich sequence within the 5'-UTR of NRAS mRNA. Notably, the synthesis of this probe is convenient and accessible. Researchers can design and synthesize their own GTFH probes for investigating the folding of specific G-quadruplex structures within RNAs of interest in cells by following the idea and application examples given in this study. The smart GTFH probe represents a novel tool for deciphering the folding of individual RNA G-quadruplex structures and understanding how G-rich RNA structures evolved within cells. Concentration-dependent experiments demonstrated the detection limit of ISCH-nras1 for NRAS RNA was about 0.1 fmol per cell (Figures S27–S28). Thus, in the present visualization approach, RNAs needed to be transfected into cells in view of the extremely low concentration of particular RNAs in a single cell. Notably, we constructed a 5'-UTR of the NRAS mRNA reporter and transfected the plasmid into cells to increase the endogenous RNA concentration. After treatment of ISCH-nras1, enhanced fluorescence could be found by quantification of cells using high-content imaging platform (Figures S29–S30), but the *in situ* detection of spots of particular RNA G-quadruplex in a single cell is still a challenge (Figure S31). The design of the GTFH probe and the collective results from this study may be the first steps to achieving this aim. Further improvements on the probe to enable the *in situ* visualization of particular G-quadruplex, including modification of the fluorescent light-up moiety and the nucleotides or length of anti-tail sequence are now underway.

■ ASSOCIATED CONTENT

📄 Supporting Information

The Supporting Information is available free of charge on the ACS Publications website at DOI: [10.1021/jacs.6b04799](https://doi.org/10.1021/jacs.6b04799).

Synthesis and characterization of the probes, experimental procedures, and supplemental spectra and graphs (PDF)

■ AUTHOR INFORMATION

Corresponding Authors

*ceshzs@mail.sysu.edu.cn

*tanjiah@mail.sysu.edu.cn

Notes

The authors declare no competing financial interest.

■ ACKNOWLEDGMENTS

This work was supported by the National Natural Science Foundation of China (81330077, 91213302, and 21272291), the Guangdong Natural Science Funds for Distinguished Young Scholar (2015A030306004), and the Guangdong Provincial Key Laboratory of Construction Foundation (2011A060901014).

■ REFERENCES

- (1) Leontis, N. B.; Westhof, E. *RNA* **2001**, *7*, 499.
- (2) (a) Licatalosi, D. D.; Darnell, R. B. *Nat. Rev. Genet.* **2010**, *11*, 75. (b) Wan, Y.; Kertesz, M.; Spitale, R. C.; Segal, E.; Chang, H. Y. *Nat. Rev. Genet.* **2011**, *12*, 641.
- (3) (a) Woodson, S. A. *Annu. Rev. Biophys.* **2010**, *39*, 61. (b) Chen, S. *J. Annu. Rev. Biophys.* **2008**, *37*, 197.
- (4) (a) Rouskin, S.; Zubradt, M.; Washietl, S.; Kellis, M.; Weissman, J. S. *Nature* **2014**, *505*, 701. (b) Gao, M.; Gnutt, D.; Orban, A.; Appel, B.; Righetti, F.; Winter, R.; Narberhaus, F.; Muller, S.; Ebbinghaus, S. *Angew. Chem., Int. Ed.* **2016**, *55*, 3224. (c) Sugimoto, Y.; Vigilante, A.; Darbo, E.; Zirra, A.; Militti, C.; D'Ambrogio, A.; Luscombe, N. M.; Ule, J. *Nature* **2015**, *519*, 491. (d) Spitale, R. C.; Flynn, R. A.; Zhang, Q. C.; Crisalli, P.; Lee, B.; Jung, J. W.; Kuchelmeister, H. Y.; Batista, P. J.; Torre, E. A.; Kool, E. T.; Chang, H. Y. *Nature* **2015**, *519*, 486.
- (5) Collie, G. W.; Haider, S. M.; Neidle, S.; Parkinson, G. N. *Nucleic Acids Res.* **2010**, *38*, 5569.
- (6) (a) Huppert, J. L.; Bugaut, A.; Kumari, S.; Balasubramanian, S. *Nucleic Acids Res.* **2008**, *36*, 6260. (b) Jayaraj, G. G.; Pandey, S.; Scaria, V.; Maiti, S. *RNA Biol.* **2012**, *9*, 81.
- (7) (a) Millevoi, S.; Moine, H.; Vagner, S. *Wiley Interdiscip. Rev.: RNA* **2012**, *3*, 495. (b) Bugaut, A.; Balasubramanian, S. *Nucleic Acids Res.* **2012**, *40*, 4727.
- (8) (a) Beaudoain, J. D.; Jodoin, R.; Perreault, J. P. *Nucleic Acids Res.* **2014**, *42*, 1209. (b) Kwok, C. K.; Balasubramanian, S. *Angew. Chem., Int. Ed.* **2015**, *54*, 6751.
- (9) Ellis, R. J.; Minton, A. P. *Nature* **2003**, *425*, 27.
- (10) (a) Xu, S.; Li, Q.; Xiang, J.; Yang, Q.; Sun, H.; Guan, A.; Wang, L.; Liu, Y.; Yu, L.; Shi, Y.; Chen, H.; Tang, Y. *Nucleic Acids Res.* **2015**, *43*, 9575. (b) Laguerre, A.; Hukezalie, K.; Winckler, P.; Katranji, F.; Chanteloup, G.; Pirrotta, M.; Perrier-Cornet, J. M.; Wong, J. M.; Monchaud, D. *J. Am. Chem. Soc.* **2015**, *137*, 8521. (c) Biffi, G.; Di Antonio, M.; Tannahill, D.; Balasubramanian, S. *Nat. Chem.* **2014**, *6*, 75. (d) Shivalingam, A.; Izquierdo, M. A.; Marois, A. L.; Vysniauskas, A.; Suhling, K.; Kuimova, M. K.; Vilar, R. *Nat. Commun.* **2015**, *6*, 8178.
- (11) Yan, J. W.; Chen, S. B.; Liu, H. Y.; Ye, W. J.; Ou, T. M.; Tan, J. H.; Li, D.; Gu, L. Q.; Huang, Z. S. *Chem. Commun.* **2014**, *50*, 6927.
- (12) (a) Jensen, E. *Anat. Rec.* **2014**, *297*, 1349. (b) Boutorine, A. S.; Novopashina, D. S.; Krasheninina, O. A.; Nozeret, K.; Venyaminova, A. G. *Molecules* **2013**, *18*, 15357.
- (13) Kumari, S.; Bugaut, A.; Huppert, J. L.; Balasubramanian, S. *Nat. Chem. Biol.* **2007**, *3*, 218.
- (14) Shim, J. W.; Tan, Q.; Gu, L. Q. *Nucleic Acids Res.* **2009**, *37*, 972.
- (15) (a) Zhang, L.; Zhou, W.; Velculescu, V. E.; Kern, S. E.; Hruban, R. H.; Hamilton, S. R.; Vogelstein, B.; Kinzler, K. W. *Science* **1997**, *276*, 1268. (b) Raj, A.; van den Bogaard, P.; Rifkin, S. A.; van Oudenaarden, A.; Tyagi, S. *Nat. Methods* **2008**, *5*, 877. (c) Komminoth, P.; Werner, M. *Histochem. Cell Biol.* **1997**, *108*, 325.
- (16) Zhang, J. Y.; Zheng, K. W.; Xiao, S.; Hao, Y. H.; Tan, Z. *J. Am. Chem. Soc.* **2014**, *136*, 1381.
- (17) (a) Hu, M. H.; Chen, S. B.; Guo, R. J.; Ou, T. M.; Huang, Z. S.; Tan, J. H. *Analyst* **2015**, *140*, 4616. (b) Marin, V. L.; Armitage, B. A. *J. Am. Chem. Soc.* **2005**, *127*, 8032. (c) Monchaud, D.; Allain, C.; Teulade-Fichou, M. P. *Bioorg. Med. Chem. Lett.* **2006**, *16*, 4842.
- (18) Xu, Y.; Kaminaga, K.; Komiyama, M. *J. Am. Chem. Soc.* **2008**, *130*, 11179.
- (19) (a) Xu, Y.; Ishizuka, T.; Yang, J.; Ito, K.; Katada, H.; Komiyama, M.; Hayashi, T. *J. Biol. Chem.* **2012**, *287*, 41787. (b) Xu, Y.; Suzuki, Y.; Ito, K.; Komiyama, M. *Proc. Natl. Acad. Sci. U. S. A.* **2010**, *107*, 14579.